A test of the viability of fluid – wallrock interaction mechanisms for changes in opaque phase assemblage in metasedimentary rocks in the Kambalda-St. Ives Goldfield, Western Australia

Evans, K.A.

School of Applied Geology, Curtin University of Technology, GPO Box U1987, Bentley, WA6845, Australia. Email: k.evans@curtin.edu.au, Telephone: 0061 8 92664682; Fax 0061 8 92663153.

Keywords: gold, pyrite, pyrrhotite, magnetite, fluid, St Ives

Abstract Transitions from pyrrhotite-magnetite- to pyrite-magnetite- and pyrite-hematite-bearing assemblages in metasedimentary rocks in the Kambalda-St Ives goldfield have been shown to be spatially associated with economic gold grades. Fluid mixing, fluid-rock interaction and phase separation have been proposed previously as causes for this association. Textural, mineralogical and isotopic evidence is reviewed, and thermodynamic calculations are used to investigate the mineralogical consequences of progressive fluid-rock interaction in interflow metasediments. Fluid-rock interactions in response to fluid infiltration and/or bulk composition variation are plausible mechanisms for production of the observed features.

Introduction

The Kambalda-St Ives goldfield, hereafter referred to as St Ives for convenience, is located in the Norseman-Wiluna greenstone belt in the Eastern Goldfields province of the Yilgarn Craton in Western Australia (Fig. 1). Around 233 tonnes of gold have been mined from St. Ives, out of a total estimated endowment of around 373 tonnes (Prendergast 2007). The deposits have been described as mesothermal (e.g., Cox and Ruming 2004) or orogenic (e.g., Neumayr et al. 2008). Gold is hosted by felsic intrusions, komatiites and, in much of the area, in basalts and differentiated dolerite sills.

A variety of mechanisms have been proposed for the deposition of gold in basaltic rocks in this group of deposits, which include fluid-wallrock interaction (Neall and Phillips 1987; Palin and Xu 2000; Hodkiewicz et al. 2009), phase separation (Palin and Xu 2000, Hodkiewicz et al. 2009), and mixing of fluids with contrasting redox states

(Neumayr et al. 2005, 2008). Each of these mechanisms involves gold deposition driven by a lowering of the concentration of reduced sulphur complexes in solution, and consequent destabilisation of aqueous gold-sulphide complexes. However, the cause of the loss of reduced sulphur from solution differs in each case. In the case of fluid:wallrock interaction, loss of sulphide from solution is caused by reaction with the wallrock to form sulphide minerals, and, in some cases, oxidation to form sulphate, which does not complex gold (e.g., Evans et al. 2006). In the case of phase separation, sulphide is partitioned into the low density phase, resulting in increased sulphate in the high density phase and gold deposition (e.g., Palin and Xu 2000, Hodkiewicz et al. 2009). And, in the case of fluid mixing, the interaction of reduced, gold-bearing fluids with oxidised fluids causes oxidation of sulphide to sulphate and gold deposition (e.g., Neumayr et al. 2008).

Evidence used to distinguish between the hypotheses includes mineral assemblages, textural relationships and sulphur isotope values in syn-mineralisation sulphides. Anomalously light sulphur isotopes (<-4 ‰) in syn-mineralisation pyrite are consistent with the presence of sulphate during gold deposition (e.g., Neumayr et al. 2008, Hodkiewicz et al. 2009), but aqueous sulphate is proposed to have been present during each of the precipitation mechanisms listed above, so sulphur isotope evidence may not be an effective way to distinguish between the gold deposition mechanisms.

Evidence that mineral assemblages record wallrock interaction is provided by increased modes of sulphide minerals in wallrock proximal to the shear zones that host gold (e.g., Neall and Phillips 1987). Additionally, gold mineralisation is commonly disseminated within the wallrock (Cox and Ruming 2004), which supports a role for the wallrock in gold deposition. On the other hand, Neumayr et al. (2008) used regional- and local-scale variation and overprinting textures in the opaque phase assemblage found in interflow sedimentary rocks at St. Ives to infer mixing between oxidised and reduced fluids. However, it has been demonstrated that similar assemblage transitions in metabasic rocks can occur simply as a result of progressive fluid-rock interaction (Evans et al. 2006).

Thermodynamic modelling provides a way to investigate the evolution of mineral assemblage as a consequence of fluid-rock interaction, and to test if such interactions can produce features attributed to fluid mixing at St. Ives. It is difficult to address gold deposition explicitly, because there is little direct evidence that can be tested with a thermodynamic model such as that used here. Additionally, quantitative simulation of phase separation is beyond the scope of the models employed for this study. The aim of this study, therefore, is to use thermodynamic modelling techniques to place quantitative constraints on the degree to which progressive fluid-wallrock interactions can cause the assemblages and textures observed in metasedimentary rocks in the St. Ives goldfield.

Geological setting

The St. Ives gold field is associated spatially with the Playa fault, which is a splay off the regional scale Boulder-Lefroy Fault. The host-rocks are a 2.71 to 2.68 Ga (Watchorn 1998) sequence of Archaean metakomatiites and metabasalts several km thick, which include minor interflow sediments (Bavinton 1981). The sequence is intruded by a number of differentiated tholeiitic sills, which can be up to 100m thick, and by younger felsic to intermediate rocks (2.65 Ga, Watchorn 1998).

In the vicinity of the Intrepide mine, gold mineralisation is hosted by komatiite and the felsic intrusions, whereas, in the vicinity of the Revenge and Victory-Defiance mines, gold is hosted in rocks of basaltic composition, and in interflow sediments such as the Kapai Slate (Prendergast 2007). Gold mineralisation occurred after the bulk of the felsic magmatism and occurs in networks of brittle-ductile shear zones, with gold preferentially hosted in altered wall-rock adjacent to veins, shear zones and faults rather in the veins and faults themselves. Information on the component deposits is provided by Phillips and Groves (1984), Clark et al. (1986), Neall and Phillips (1987), Watchorn (1998), Palin and Xu (2000), Petersen et al. (2005), Neumayr et al. (2005) and Neumayr et al. (2008).

Mineral assemblages

Studies of the St. Ives area (e.g., Neall and Phillips 1987; Palin and Xu 2000; Neumayr et al. 2005; Neumayr et al. 2008; Hodkiewicz et al. 2009) have noted variability in the distribution of the iron oxide and sulphide phases in the interflow sediments on cm to km scales (e.g., Neumayr et al. 2008, Fig. 1). On a 10 km scale, pyrite-rich assemblages are common in the north of the area around the Revenge deposit, and at the southern margin of the Victory-Defiance group of deposits. Pyrite-pyrrhotite dominates at the Hunt Mine, and in most of the central region, with the exception of narrow km-scale domains in which magnetite is the dominant opaque phase. It has been proposed that the magnetite-rich zones are associated with gravity lows, which are inferred to be caused by felsic intrusions at depth. On a deposit scale, transitions between the opaque phase assemblages have been correlated with economic gold grades (e.g., Neumayr et al. 2008).

Textural observations include pre- to early syn-mineralisation magnetite growth in mafic rocks adjacent to gold lodes (Neumayr et al. 2008) and destruction of magnetite in mafic rocks during gold mineralisation (Neall and Phillips 1987; Watchorn 1998; Palin and Xu 2000; Neumayr et al. 2008). At Revenge, magnetite inclusions are recorded in the cores of gold-related pyrite grains which include hematite at the rim (Neumayr et al. 2008), though the composition of the host rock for this texture is not noted. At Conqueror, which is one of the Victory-Defiance group of deposits, Neumayr et al. (2008) document apparently synchronous formation of pyrrhotite inclusions in pyrite and pyrite inclusions in pyrrhotite, in samples from fractures in different orientations. Carbonate alteration is well documented (Neall and Phillips 1987; Watchorn 1998; Palin and Xu 2000). The presence of iron-bearing calcite, ankerite, and, in some cases, siderite, accompanies changes in the opaque phase assemblage from magnetite-pyrrhotite to magnetite-pyrite and pyrite-hematite.

Conceptual model

Simple end-member reactions can be used to link the observed carbonation to changes in the opaque phase assemblage (c.f., Phillips and Brown 1987), e.g.,

$$Fe_3O_4 + CO_2 = Fe_2O_3 + FeCO_{3(ss)}, \qquad [1]$$

and

$$Fe_3O_4 + 2FeS + 4CO_2 = FeS_2 + 4FeCO_{3(ss)}, \qquad [2]$$

where the $FeCO_3$ need not be siderite but may be an iron-bearing component in ankeritic dolomite or calcite, as indicated by the subscript ss. These reactions are highly simplified; additional Fe^{3+} is likely to have been held by silicate phases such as chlorite, epidote, and amphibole, and Fe^{2+} liberated by magnetite breakdown could have transferred to hydrothermal silicate phases such as chlorite. Nevertheless, these reactions are consistent with observed mineralogical changes and demonstrate that formation of hematite and pyrite may occur without influx of an oxidising fluid.

The sulphate-forming reaction can also be driven by magnetite breakdown without any need for an external oxidant, e.g.,

$$4Fe_3O_4 + H_2S + 12CO_2 = H_2SO_4 + 12FeCO_{3(ss)}. \qquad [3]$$

Gold deposition at the interface between different sulphide/oxide assemblages are consistent with this model, because gold solubility is controlled by fluid characteristics such as pH, redox state, and sulphur concentration, and these parameters change sharply with transitions in the sulphide/oxide assemblage. High gold grades in Ti-rich fractionated dolerite sills (e.g., Prendergast 2007) in the St. Ives gold camp may also support the proposal that reactions [1] to [3] played an important role in gold deposition. High Ti commonly accompanies high magmatic magnetite contents, so the high Ti-rocks have the greatest oxidising capacity and thus a high probability that reactions [1] to [3] are driven to the extent that changes in sulphide/oxide assemblages induce deposition of gold from solution.

Thus, documented mineral assemblages, gold grades, and sulphur isotope compositions can be produced by reactions [1] to [3], if these reactions occurred to a sufficient extent and at appropriate pressures and temperatures. This issue is explored with thermodynamic modelling below.

Thermodynamic modelling

All calculations presented here were made using the program HCh (Shvarov and Bastrakov 1999); also see Oliver et al. (2004) and Evans et al. (2006). HCh is chosen for thermodynamic modeling because it can calculate mineral assemblages and modes, and the compositions of coexisting fluids and mineral assemblages for compositionally complex rocks and at the pressures and temperatures of interest, and can be used to mimic open system behaviour. However, there are some limitations to the software. The principal of these is that HCh lacks the algorithms necessary to calculate the thermodynamic properties of phases that mix non-ideally, e.g., CO_2-rich fluids or complex mineral solid solutions such as chlorite. Nevertheless, predicted sequence of mineral assemblages and relative modes are likely to be robust. The system investigated here is Na_2O-CaO-K_2O-FeO-MgO-Al_2O_3-SiO_2-CO_2-O-S-H_2O. The database utilised was the Unitherm database (Shvarov and Bastrakov, 1999) which is distributed with HCh.

The bulk composition considered (Table 1) is based on the average composition (Bavinton 1981) for interflow sedimentary rocks associated with nickel sulphide deposits in the Kambalda-St. Ives region. The compositions are modified by a reduction in the mode of sulphides and graphite, because the values recorded by Bavinton (1981) are very high (12 wt% pyrrhotite, 5 wt% pyrite, 1 wt% carbon) and are unlikely to represent of the interflow sediments on a regional scale. However, other components such as SiO_2 are typical of those found in Archaean metasedimentary rocks (Bavinton 1981) and are used without modification. Fe^{3+}:Fe^{2+} ratios for these rocks are not recorded, so a range of bulk Fe^{3+}:Fe^{2+} was tested for the model. The results shown were acquired for a bulk 35% Fe^{3+}, which is within the range of plausible values. The effect of the assumed bulk contents of S, C and Fe^{3+} on results are discussed below. All models were calculated at an assumed pressure of 0.2 GPa, which is consistent with those calculated for St. Ives (e.g., Hodkiewicz et al. 2009).

Two conceptual models were investigated. Model 1 is of a system with fixed bulk composition, including water and CO_2, which can be imagined as a sealed box that contains rock and fluid. Mineral assemblages and modes were calculated for this composition at a sequence of temperatures at fixed pressure. This model is simplistic because it is a closed system, whereas open systems are necessary to form ore deposits. Additionally, temperature changes are not thought to be a major driver of gold deposition in orogenic gold deposits at the deposit scale (e.g., McCuaig and Kerrich, 1998). However, the model is valuable because it demonstrates the magnitude of changes in opaque phase assemblage that can be driven without any addition of an oxidising fluid i.e. without any change in the extensive redox variable. The volatile content of the system was 8.5% by weight, which reflects a small to moderate total fluid:rock ratio. Initial $X(CO_2)$ was 0.21 but this varied in the range 0.1 to 0.4 as mineral carbonation and hydration proceeded with changing temperature.

Model 2 mimics a rock that is progressively altered by aliquots of infiltrating fluid at fixed temperature and pressure. This model is more realistic, physically, than Model 1 because it simulates more closely the open systems that are likely to have operated during mineralisation at St. Ives. The starting rock bulk composition, which is the same as for Model 1, was successively equilibrated with small increments (0.7% of the rock mass) of a H_2O-CO_2-NaCl-H_2S fluid similar to those inferred for St Ives (Petersen et al. 2006; $X(CO_2)=0.13$, $X(H_2S)=0.01$, NaCl = 5.4 wt%) at the temperature and pressure of interest. After each equilibration step, the fluid was removed and a fresh aliquot of fluid was added, so that the fluid:rock ratio at any given time was always small and approached physically plausible values. It is assumed that alteration at St. Ives was progressive. That is, the precursors to the rocks in the highly altered zones proximal to the gold lodes were the same as those in the less altered rocks distal to the lodes at an earlier stage of the evolution of the proximal zone. Under this assumption, Figs. 2B and C represent a cross-section through the alteration zones, from distal (low cumulative fluid:rock ratio) to proximal (high fluid:rock ratio).

Results

Model 1

Calculated silicate and carbonate mineral assemblages (not shown in Figure 2) comprise ankerite, chlorite, albite, muscovite and quartz, plus epidote at temperatures higher than 440^{o}C and siderite below 280^{o}C. These minerals are typical of those seen in metasedimentary rocks in the St. Ives region (Bavinton 1981) and lend credence to the ability of the model to provide information on the gold-forming event. Biotite is not predicted though it is observed in some of the metasedimentary rocks. The most likely cause for this is the lack of appropriate activity-composition models in HCh, however, the omission does not affect the conclusions of this paper. Principal features of interest are, from high to low temperature: (1) the absence of pyrrhotite below 400^oC; (2) the change from a dominant aqueous S^{2-} sulphur species to a dominant aqueous S^{6+} sulphur species between 300 and 350^oC, which would drive the formation of isotopically light sulphide minerals; and (3) the change from magnetite to hematite between 300 and 270^oC. These changes do not require input of an oxidising fluid because they are driven by carbonation and breakdown of magnetite, i.e. by reactions [1] to [3].

Model 2

Predicted silicate assemblages (not shown) are consistent with those observed in the field and comprise amphibole (ferrotremolite), chlorite, carbonates, epidote, K- and Na-micas and feldspar (albite and microcline). Results are shown for 300 and 350^oC.

At 300^oC (Fig. 2B), progressive fluid:rock interaction drives the oxide-sulphide assemblage from magnetite-pyrite-pyrrhotite, to magnetite-pyrite, to hematite-pyrite, to hematite-pyrite-magnetite, and then back to pyrite-magnetite. The changes are driven by transfer of Fe^{3+} from magnetite to hematite i.e. by reactions [1] to [3], then hematite is lost as Fe^{3+} is consumed by the oxidation of aqueous S^{2-} to S^- in pyrite. The formation of aqueous sulphate, which is driven by the reduction of hematite and magnetite-hosted Fe^{3+}, would facilitate the formation of isotopically light sulphide minerals.

Comparable features are observed at 350^oC (Fig. 2C). Progressive addition of H_2O-CO_2-NaCl-H_2S fluid drives the oxide-sulphide assemblage from magnetite-pyrite-pyrrhotite, to magnetite-pyrite, and then back to magnetite-pyrite-pyrrhotite. The appearance, disappearance, and reappearance of pyrrhotite reflects the competing influences of the decreasing Fe:S ratio as S is added to the rock, and consumption of Fe^{3+} by oxidation of S^{2-} in pyrrhotite to S^{-} in pyrite. Aqueous sulphate forms at this temperature, but at a lesser extent than at 300^{o}C, so the associated sulphides would not necessarily be anomalously isotopically light.

The effects of increasing the redox budget of the modelled bulk, by decreasing S and increasing Fe(III), were to increase the mode of magnetite, broaden the stability field of hematite and aqueous sulphate, stabilise anhydrite, and to reduce the stability field of pyrrhotite. Conversely, a decreased redox budget, in the form of increased S, C and reduced Fe(III) destabilised hematite, magnetite and aqueous sulphate, and increased the stability field of pyrrhotite.

Discussion

The model results demonstrate that either temperature gradients or progressive fluid-rock interaction can produce a range of opaque phase assemblages without any requirement for multiple fluids. However, the relatively restricted spatial distribution of the different mineral assemblages is not consistent with a first-order temperature control.

Textures noted by Neumayr et al. (2008) are predicted as a consequence of progressive fluid-rock interaction. Hematite growth follows magnetite at 300^{o}C (Fig. 2B) and simultaneous growth of pyrite inclusions in pyrrhotite and pyrrhotite in pyrite could occur in neighbouring rocks with different extents of fluid-rock interaction (Fig. 2C).

Early magnetite growth in metabasic rocks is predicted by models similar to those presented here as a consequence of the transfer of Fe(III) from amphibole to magnetite (results not shown).

On a km-scale, the results are consistent with observations in the vicinity of the Victory-Defiance group of deposits, where magnetite is recorded directly above an inferred km-wide intrusion, and pyrrhotite-dominated assemblages are recorded peripheral to the intrusion. Figs. 2B and C show that pyrrhotite is present at relatively low degrees of fluid-rock interaction, but is replaced by pyrite and magnetite with increasing fluid:rock ratio, which might be expected close to intrusions if intrusion-related fracturing created high permeabilities.

The HCh model results also indicate that small variations in the C and S content of the interflow sediments can change the stable opaque phase assemblage. Neumayr et al. (2008) state that the interflow sediments are of homogeneous bulk composition, however relatively little variation is needed to produce the effects described. Such variation can be due to depositional, diagenetic or metamorphic causes, for example, pre-mineralisation fluid flow related to the intrusion could have removed C and S from the interflow sediments, with consequent stability of magnetite at a later date. Without detailed bulk composition data it is impossible to quantify the relative roles of bulk composition and fluid:rock interaction. However, such studies may prove worthwhile in the future.

A feature unaccounted for by the model is the albite-hosted, water-poor fluid inclusion compositions reported by Petersen et al. (2005,2006). Fluids in these inclusions are CO_2-rich, with methane up to 5 mole %. Such fluids can be produced by phase-separation, the presence of a discrete carbonic fluid, or by selective post-entrapment water-loss from the albite-hosted inclusions. The densities of the water-poor inclusions are less than those of associated carbonate-hosted inclusions, which supports the latter hypothesis.

Conclusions

This contribution has shown that carbonation and destruction of minerals that contain ferric iron, such as magnetite via reactions [1] to [3], can produce hematite, sulphate and stabilise pyrite over pyrrhotite without any need for an external source of oxidation. Mixing of fluids with contrasting redox states or phase separation are not required, however, a role for these processes is not precluded by the evidence presented here. Kilometre- to micron-scale changes in sulphide-oxide assemblage in metasedimentary rocks observed at St. Ives are consistent with changes in the extent of fluid:rock interaction, and variation in host-rock bulk composition caused by depositional, diagenetic or pre-mineralisation metamorphic factors.

Acknowledgements This work was supported by a Curtin University Research and Teaching Fellowship and by CSIRO (Commonwealth Scientific and Industrial Research Organisation) Exploration and Mining. Neil Phillips and Roger Powell are thanked for helpful discussions. Frank Bierlein is thanked for a perceptive review that improved the paper, and Patrick Williams is thanked for editorial support.

References

Bavinton OA (1981) The nature of sulfidic metasediments at Kambalda and their broad relationships with associated ultramafic rocks and nickel ores. Econ Geol 76:1606 – 1628

Cox SF, Ruming K (2004) The St Ives mesothermal gold system, Western Australia – a case of golden aftershocks? J Struct Geol 26:1109 – 1125

Evans KA, Phillips GN, Powell R (2006) Rock-buffering of auriferous fluids in altered rocks associated with the Golden Mile-style mineralization, Kalgoorlie gold field, Western Australia. Econ. Geol 101: 805 – 817

Hodkiewicz PF, Groves DI, Davidson GJ, Weinberg RF, Hagemann SG (2009) Influence of structural setting on sulphur isotopes in Archean orogenic gold deposits, Eastern Goldfields province, Yilgarn, Western Australia. Miner Depos 44:129 – 150

McCuaig TC, Kerrich R (1998) P-T-t-deformation-fluid characteristics of lode gold deposits: evidence from alteration systematics. Ore Geol. Rev. 12: 381– 453.

Neall FB, Phillips GN (1987) Fluid-wall interaction in an Archean hydrothermal gold deposit: a thermodynamic model for the Hunt Mine, Kambalda. Econ. Geol. 82: 1679 – 1694

Neumayr P, Petersen KJ, Gauthier L, Hodge JL, Hagemann SG, Walshe JL, Prendergast K, Connors K, Horn L, Frikken P, Roache A, Blewett RS (2005) Mapping of hydrothermal alteration and geochemical gradients as a tool for conceptual targeting: St. Ives Gold Camp, Western Australia. In: Bierlein FP, Mao J (eds) Mineral Deposit Research: Meeting the Global Challenge. Springer, Berlin, pp 1479 – 1482

Neumayr P, Walshe J, Hagemann S, Petersen K, Roache A, Frikken P, Horn L, Halley S (2008) Oxidized and reduced mineral assemblages in greenstone belt rocks of the St. Ives gold camp, Western Australia: vectors to high—grade ore bodies in Archaean gold deposits? Miner Depos 43: 363 – 371

Oliver NHS, Cleverley JS, Mark G, Pollard PJ, Fu B, Marshall LJ, Rubenach MJ, Williams PJ, Baker T (2004) Modeling the role of sodic alteration in the genesis of iron oxide-copper-gold deposits, Eastern Mount Isa block, Australia. Econ Geol 99: 1145 – 1176

Palin JM, Xu Y (2000) Gilt by association? Origins of pyritic gold ores in the Victory mesothermal gold deposit, Western Australia. Econ Geol 95: 1627 – 1634

Petersen KJ, Neumayr P, Hagemann SG, Walshe JL (2005) Paleohydrologic evolution of the Kambalda gold camp. In: Bierlein FP, Mao J (eds) Mineral Deposit Research: Meeting the Global Challenge. Springer, Berlin, pp 573 – 576

Petersen KJ, Neumayr P, Walshe J, Hagemann S (2006) Types of fluid compositions and evolution at the St. Ives gold camp. Geochim et Cosmochim Acta 70:A485 – A485

Prendergast K (2007) Application of lithogeochemistry to gold exploration in the St Ives goldfield, Western Australia. Geochem-Explor Environ An 7:99 – 108

Phillips GN, Groves DI (1984) Fluid access and fluid-wall rock interaction in the genesis of the Archaean gold-quartz vein deposit at Hunt Mine, Kambalda, Western Australia. In: Foster RP (ed) Gold ’82: the geology, geochemistry and genesis of gold deposits. A.A. Ba;kema, Rotterdam, pp389 – 416

Phillips GN, Groves DI, Neall FB, Donnelly TH, Lambert IB (1986) Anomalous sulfur isotope compositions in the Golden Mile, Kalgoorlie. Econ Geol 81:2008 – 2015

Phillips GN, Brown IJ (1987) Host rock and fluid control on carbonate assemblages in the Golden Mile Dolerite, Kalgoorlie gold deposit, Australia. Canad Min 25: 265 – 273.

Prendergast K (2007) Application of lithogeochemistry to gold exploration in the St Ives goldfield, Western Australia. Geochem-Exp Environ Analysis 7:99 – 108

Shvarov Y, Bastrakov E (1999) HCh: a software package for geochemical equilibrium modelling. User's Guide. Australian Geological Survey Organisation, Canberra. Record 1999/25; 61pp.

Watchorn RB (1998) Kambalda-St. Ives gold deposits. In: Berkman DA, Mackenzie DH (eds) Geology of Australian and Papua New Guinean mineral deposits. The Australasian Institute of Mining and Metallurgy, Melbourne, pp 243 – 254.

Table 1: Fluid and rock compositions used to produce Fig. 2.

Rock	
Component	wt %
SiO_2	56.42
Al_2O_3	12.60
FeO	6.51
Fe_2O_3	5.07
MgO	3.15
CaO	4.08
Na_2O	1.98
K_2O	2.48
FeS_2	3.55
H_2O	2.08
CO_2	2.08
Model 2 fluid	
Component	Mole %
H_2O	84
CO_2	13
NaCl	2
H_2S	1

Figure Captions

Fig. 1. Map of parts of the Yilgarn, with inset showing selected deposits at St. Ives. After Evans et al. (2006) .

Fig. 2. Modes of opaque mineral phases calculated with HCh. Rock bulk and fluid compositions are shown in Table 1, pressure = 0.2 GPa. p(ox) refers to the proportion of oxidised sulphur, equal to $S^{6+}/(S^{6+}+S^{2-}+S^{-})$ where concentrations are molal. Model 1 – rock equilibrated with 8.5% fluid by weight at 250 – 450 ^{o}C in a closed system. Decreasing temperature stabilises pyrite over pyrrhotite, then hematite over magnetite, and stabilises sulphate in solution. B. Effects of progressive fluid infiltration in an open system at 300^{o}C. Pyrrhotite is destabilised, and hematite and sulphate stabilised, and then destabilised, with increasing extent of fluid-rock interaction. C. Effects of progressive fluid infiltration in an open system at 350^{o}C. Pyrrhotite first reacts out, then reacts back in again, with increasing extent of fluid-rock interaction.

Evans et al. Figure 1.

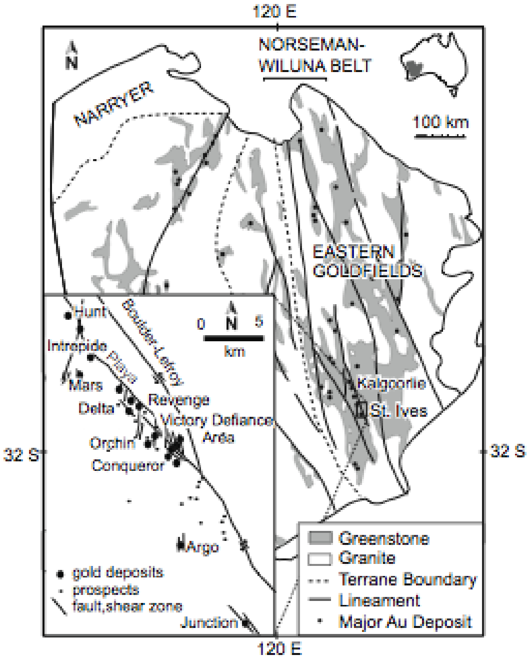

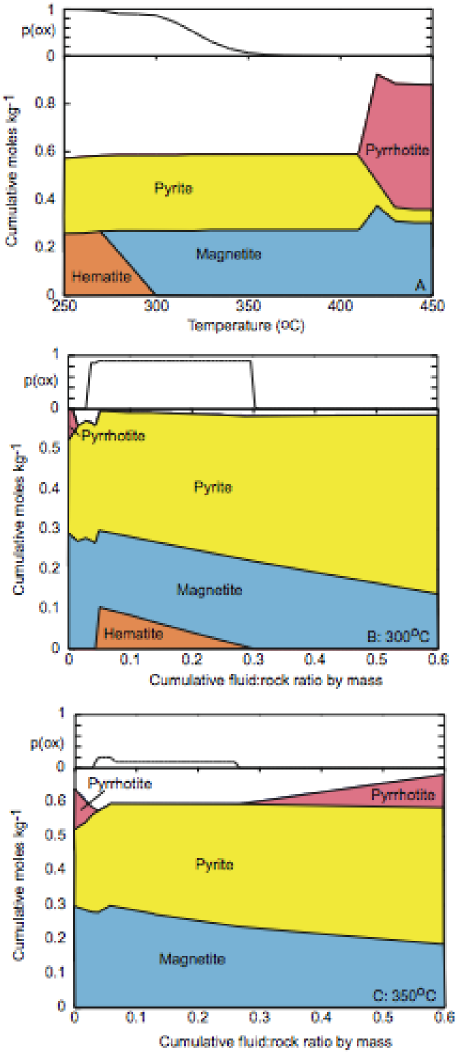

p(ox)
1
0
Cumulative moles kg-1
0.8
0.6
0.4
0.2
0
Pyrrhotite
Pyrite
Magnetite
Hematite
A
250
300
350
400
450
Temperature (oC)
p(ox)
1
0
Cumulative moles kg-1
0.5
0.4
0.3
0.2
0.1
0
Pyrrhotite
Pyrite
Magnetite
Hematite
B: 300oC
0
0.1
0.2
0.3
0.4
0.5
0.6
Cumulative fluid:rock ratio by mass
p(ox)
1
0
Cumulative moles kg-1
0.6
0.5
0.4
0.3
0.2
0.1
0
Pyrrhotite
Pyrrhotite
Pyrite
Magnetite
C: 350oC
0
0.1
0.2
0.3
0.4
0.5
0.6
Cumulative fluid:rock ratio by mass